THE JOURNAL OF PHYSICAL CHEMISTRY B

ARTICLE

pubs.acs.org/JPCB

On the Structure Selectivity of Clathrate Hydrates

Masakazu Matsumoto* and Hideki Tanaka

Graduate School of Natural Science and Technology, Okayama University, 3-1-1 Tsushima, Okayama 700-8530, Japan

ABSTRACT: We propose a strategic method to search for a new clathrate hydrate by investigating the selectivity of its crystalline structure, which has been expected to depend mostly on the guest species and less on the thermodynamic conditions. Relative stability among various morphologies is examined in terms of the chemical potential of water of clathrate hydrates in equilibrium with guest gases. This evaluation is performed by calculating the free energy of cage occupancy according to the standard statistical mechanical theory with the aid of the Yarmolyuk and Kripyakevich's rule on the Frank-Kasper type alloys to estimate the numbers of cages of various types. Thus, a comprehensive interpretation of the selectivity of crystalline structures is successfully made. We explain why two major structures are stable in most of the thermodynamic conditions and establish a relation between polymorphism of clathrate hydrate and the guest size and other parameters, thereby suggesting a way to find a new clathrate hydrate by appropriate choice of the guest species and/or the thermodynamic properties. It is found that there is a small room in the above parameter space for the other structure than the major two to be the most stable, including a new structure. In addition, simple but thorough elucidation is given for preferential formation of TS-I structure in bromine hydrate.

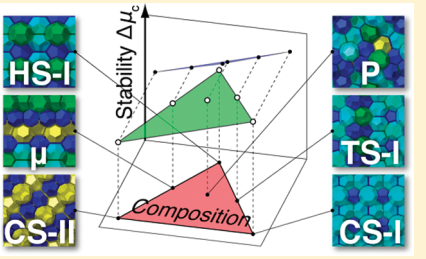

I. INTRODUCTION

Clathrate hydrate is a solid solution of water encaging the hydrophobic guest molecules in its cage-like cavities.[1] Methane hydrate is the most promising one as a future energy resource on account of its abundance in nature among many hydrates containing small hydrophobic molecules that form the clathrates with water.[2] It is also expected as an environment-friendly heat reservoir material because of its large heat capacity. On the other hand, a mixture of gas and water forms a solid hydrate under a certain thermodynamic condition, which causes serious hindrance to the flow of natural gas by blocking pipelines. A knowledge on the thermodynamic stability and the physical properties of clathrate hydrates of various structures has been awaited.

It is well-known that almost all of the clathrate hydrates are in either CS-I or CS-II structure, which is usually called simply as structures I or II, depending on the size of the guest gas molecule.[2] Few exceptions include bromine and dimethyl ether hydrate in TS-I structure,[3,4] metastable Xe hydrate in HS-I structure,[5] hydrates accommodating very large guest molecules in HS-III structure (also known as structure H),[2] and hydrates under very high pressure.[2,6] A cage in a clathrate hydrate is a polyhedron composed of 20−28 water molecules and typically one guest molecule is encapsulated in it. Water molecules and hydrogen bonds (HBs) constitute the vertices and the edges of the polyhedron, respectively. In clathrate hydrates, one vertex is shared by four cages, i.e., every water molecule is coordinated by four guest molecules, which is in turn due to the tetrahedral local arrangement of water molecules maintained even with the existence of a hydrophobic gas molecule.[7] Thus, the cages are tetrahedrally close-packed (TCP) everywhere in a clathrate hydrate.

Frank and Kasper discussed the correspondence between the arrangement of the cages in inert gas hydrates and that of the atoms in alloys of TCP structure which are now called "the Frank-Kasper (FK) structures".[8] Arrangement of the guest molecules in the CS-I, CS-II, HS-I, and TS-I clathrate structures is indeed identical to the atomic arrangement in the FK structures, A15, C15, Z, and σ, respectively. There are, however, many other crystalline structures in FK structures,[9] and one can therefore construct the corresponding hypothetical clathrate hydrate structures by applying the atomic arrangement in the FK structures. It is tempting to examine whether one can design the unknown clathrate hydrate structures based on the method proposed by Frank and Kasper.[8] In the present work, we focus on the Frank-Kasper type clathrate hydrates, i.e., those having the cages consist of pentagonal and hexagonal faces only.

It is known that a clathrate hydrate of gas mixture sometimes forms a crystal structure different from the crystal structure each component gas prefers. For example, the gas mixture of methane and ethane at a specific composition forms CS-II structure even though both pure methane and ethane gas prefer CS-I structure.[10] The structure is supposed to be stabilized when the size of the guest molecule and the composition fit to the size and composition of the cages. It is therefore expected that mixing of gases might yield new crystal structures which are different from those for the major clathrate hydrates.

Our goal in the present study is 2-fold. One is to examine whether stable clathrate hydrates are indeed realized derived from the FK structures with a reasonable water−water interaction. The other is to provide a prescription to find a possible new structure that might be stabilized in the presence of a specific guest molecule

Received: April 14, 2011
Revised: May 27, 2011
Published: May 28, 2011

Table 1. Number of the Cages (N_k) and Water (N_w) in the Simulation Cells and Their Sizes

FK[a]	CH[a]	N_w	N_{12} (α_{12}[b])	N_{14} (α_{14})	N_{15} (α_{15})	N_{16} (α_{16})	cell/Å	refs
A15	CS-I	368	16 (1/23)	48 (3/23)	0	0	a = 24.06	c
C15	CS-II	136	16 (2/17)	0	0	8 (1/17)	a = 17.31	d
Z	HS-I	640	48 (3/40)	32 (1/20)	32 (1/20)	0	a = 24.32	e
							b = 42.13	
							c = 23.35	
σ	TS-I	344	20 (5/86)	32 (4/43)	8 (1/43)	0	a = 23.18	f
							c = 24.29	
μ		592	56 (7/74)	16 (2/74)	16 (2/74)	16 (2/74)	a = 24.46	g
							b = 21.18	
							c = 44.28	
P		320	24 (3/40)	20 (1/16)	8 (1/40)	4 (1/80)	a = 23.45	g
							b = 23.18	
							c = 22.36	
	Ice Ih	360					a = 22.79	h
							b = 23.67	
							c = 22.33	

[a] FK and CH indicate the crystal name in Frank-Kasper and clathrate hydrate nomenclatures, respectively. [b] The number of cages per a water molecule, i.e., N_k/N_w. [c] Reference 13. [d] Reference 14. [e] The cell size at 273 K is determined from the data in ref 5 by applying the typical linear thermal expansion coefficient of ice analogues, (6×10^{-5} K^{-1}) [ref. 2]. [f] The cell size at 273 K is determined from the data at 173 K in ref 4 in the same way as e. [g] Obtained from Alloy database and scaled so as to reproduce the first peak distance of oxygen−oxygen radial distribution function of other clathrate hydrate crystals. [ref 15]. [h] Reference 16.

which has the highest adaptability to the given cages. In this article, the selection rules for the gas clathrate structures are established and the possibility of designing the undiscovered crystal structures is discussed.

II. THEORIES

A. Hypothetical Clathrate Hydrate Structures. A close-packing of four spheres in regular-tetrahedral arrangement permits the highest density in the local structure.[11] A crude packing of five regular tetrahedra, however, yields a pentagonal bipyramid with a small gap, which results in the global geometrical frustration when a large number of tetrahedra are packed together.[12] In FK structures, a small distortion to the shape of tetrahedra is allowed to avoid the geometrical frustration, and both pentagonal and hexagonal bipyramid structures are allowed for local packing. A combination of these structures permits four kinds of different local coordination structures, that is 12-, 14-, 15-, or 16-hedral configurations. They are called FK polyhedra.[8]

As mentioned previously, there is a one-to-one correspondence between the clathrate hydrate structures (except for high pressure phases) and the FK structures of alloy. For example, the atomic arrangement in the typical FK structures, A15, C15, Z, and σ, is identical to the cage arrangement in clathrate hydrate type CS-I, CS-II, HS-I, and TS-I, respectively. We call the clathrate hydrate structures derived from the FK structures, including those are not discovered in reality, FK-based clathrate hydrate (FKCH) structures.

In the present study, crystal structures of ice and 6 kinds of FKCH (CS-I = A15 equivalent, CS-II = C15 equivalent, HS-I = Z equivalent, TS-I = σ equivalent, μ equivalent, and P equivalent) are generated. The simulation cells are all cuboid and contain one to eight unit cells of the crystal. In order to avoid a possible error associated with the proton-disorder in the finite sized cell, at least 100 sets of configurations having different proton-ordering are prepared for obtaining the thermodynamic properties averaged over all configurations. In an individual configuration, the net polarization due to the proton-disorder is constrained to zero. Basic structural and topological information of the simulation cell in the present work are listed in Table 1.

B. van der Waals−Platteeuw Theory. Stability of each crystal structure is estimated by the generalized van der Waals and Platteeuw (vdWP) theory.[14,17] It has frequently appeared in the studies on the stability of clathrate hydrates and will therefore be explained here only briefly.[13,14,16] The chemical potential of water is approximated in the framework of classical statistical mechanics under the following three assumptions: (1) the guest−guest interaction is ignored, (2) the changes of the host lattice influenced by the guest is also ignored, and (3) each cavity is occupied by at most one guest molecule. Owing to these assumptions, the grand partition function can be simply written as the product of the partition functions of hypothetical empty clathrate hydrate with N_k k-hedral cages in the unit cell and of the guest species j of the chemical potential, μ_j, in the cages as

$$\Xi = \exp(-\beta A_w^0) \prod_k \left[1 + \sum_j \exp(\beta(\mu_j - f_j^k)) \right]^{N_k} \quad (1)$$

where A_w^0 indicates the free energy of the hypothetical empty clathrate hydrate, f_j^k stands for the free energy of cage occupancy by the guest species j in the k-hedral cage, k runs over the possible types of cage, and β is the inverse of the Boltzmann constant, k_B, times temperature T.[17]

The free energy of cage occupancy f for a spherical gas molecule is defined by[14]

$$f = -k_B T \ln[(mk_B T/2\pi\hbar^2)^{3/2} \int_{V_{cage}} \exp(-\beta w(\mathbf{r}))\, d\mathbf{r}] \quad (2)$$

where m is the mass of the guest molecule and the guest-lattice interaction is given by $w(\mathbf{r})$ where $\hbar$ is the Dirac's constant. The integration is carried out inside a single cage. The f value represents the "fitness" of a gas molecule to the specific cage.

dx.doi.org/10.1021/jp203478z |J. Phys. Chem. B 2011, 115, 8257–8265

Table 2. LJ Parameters of the Guest and Host Molecules

	ε/kJ mol^{-1}	σ/Å	refs
Ar	0.9977	3.405	18
Me	1.2355	3.758	13
Xe	1.9205	4.047	18
Et	1.736	4.52	10
TIP4P	0.6487	3.154	19

The guest species examined here are treated as spherical molecules whose interaction sites coincide with their centers of mass unless otherwise mentioned.

The chemical potential of the gas, μ_j, of guest species j is approximated to that of the ideal gas as

$$\mu_j = -k_B T \ln\left(\left(\frac{2\pi m_j k_B T}{h^2}\right)^{3/2} \frac{k_B T}{p_j}\right) \quad (3)$$

in which the partial pressure p_j can be given as an independent variable. The chemical potential of water, μ_c, is derived from the grand partition function Ξ of N_w water molecules as follows:

$$\begin{aligned} \mu_c &= -k_B T \frac{\partial \ln \Xi}{\partial N_w} \\ &= \mu_c^0 + \Delta\mu_c \end{aligned} \quad (4)$$

where μ_c^0 is the chemical potential of water in the hypothetical empty hydrate and $\Delta\mu_c$ is the contribution from the guest−lattice interaction. The latter quantity $\Delta\mu_c$ is further expanded as

$$\frac{\Delta\mu_c}{k_B T} = -\frac{\partial \ln \Xi'}{\partial N_w} = -\sum_k \alpha_k \ln[1 + \sum_j \exp(\beta(\mu_j - f_j^k))] \quad (5)$$

where α_k is the number of k-hedral cages per the number of water molecule in a unit cell, i.e., N_k/N_w.

The occupancy of a cage, y, is given by the chemical potential of the guest in a gaseous state, μ, and the free energy of cage occupancy, f, as

$$y = \frac{\exp(\beta(\mu - f))}{1 + \exp(\beta(\mu - f))} \quad (6)$$

C. Free Energy of Cage Occupancy. The first term in the chemical potential of water in eq 4 is independent of the choice of the guest molecule. Structure selectivity by the gas species is therefore dependent mainly on the second term which comes from the guest−host interaction, i.e., cage occupancy. We first examine how the free energy of cage occupancy, f, depends upon the choice of the clathrate hydrate structure and the guest molecules. The water−water interaction is described by the TIP4P model.[19] The guest−host interactions are represented by Lennard-Jones (LJ) potentials assuming the Lorentz−Berthelot rule with the appropriate LJ parameters for guests. A polyatomic guest molecule such as methane and ethane is approximated to a spherical single interaction site except bromine which is discussed in the later section. The interaction parameters are listed in Table 2. All of the calculations are carried out at T = 273 K and at pressure p = 10 MPa. The free energy of cage occupancy by the guest molecules is calculated for various sizes of cages in typical clathrate hydrate crystals by eq 2 and are listed in Table 3. It indicates that the free energy of cage occupancy is dependent significantly on the type of cage in which a guest molecule is encaged but that it hardly depends on the type of crystal structure. The free energy of cage occupancy for individual crystal type is therefore approximated for simplicity by a standard value in the following manner.

Table 3. Free Energies of Cage Occupancy for Various Cage Sizes and Various Guest Molecules at 273 K

			f_{12}	f_{14}	f_{15}	f_{16}
A15	CS-I	Ar	−30.07	−31.11		
		Me	−28.14	−30.66		
		Xe	−36.88	−43.08		
C15	CS-II	Ar	−30.07			−31.77
		Me	−28.04			−31.58
		Xe	−36.55			−44.53
Z	HS-I	Ar	−30.07	−30.87	−31.33	
		Me	−28.15	−30.35	−31.05	
		Xe	−36.95	−42.76	−43.83	
Std. cage		Ar	−30.18	−31.55	−31.84	−31.96
		Me	−27.57	−31.28	−31.76	−31.88
		Xe	−34.60	−43.90	−44.90	−45.04

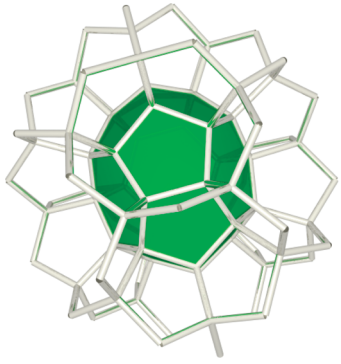

Figure 1. 15-hedron dressed by 5-membered rings illustrating the range of the guest−host interaction for calculation of the standard free energy of cage occupancy. Only the water molecules on the vertices of this image interact with the guest molecule in the central cage.

The guest molecule interacts with the oxygen atoms of water molecules on the host lattice with short-ranged LJ interaction. The dominant contribution to the guest−host interaction arises from the water molecules of the cage in which the guest is contained, called "primary cage". We therefore limit the calculation of the guest−host interaction up to the water molecules on the neighbor rings which shares one of its edge with the primary cage, i.e., to the third coordination shell of water. In the actual crystal structures, the ring is either pentagon or hexagon, but we regard all of the rings as pentagons for simplicity. Thus we obtain "a polyhedral cage decorated by pentagons" (Figure 1). The shape of the pentagon-decorated cage is optimized so that the HB oxygen−oxygen distance coincides with that of ice and the oxygen−oxygen−oxygen angle becomes closer to the tetrahedral angle, 109.5°. The pentagon-decorated 12-, 14-, 15-, and 16-hedral cages are generated and the standard free energies of cage occupancy are calculated for them. Table 3 also tabulates the standard free energy of cage occupancy, which represents the free energy of cage occupancy for guest molecules in the actual crystal structures with good accuracy. The approximated free energies thus obtained are used instead in the following analyses.

dx.doi.org/10.1021/jp203478z |J. Phys. Chem. B 2011, 115, 8257–8265

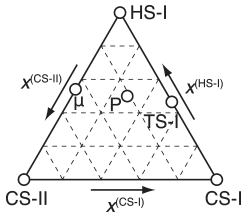

Figure 2. Compositions of six FKCH structures in the triangular diagram where three vertices correspond to the representative structures.

D. Universal Rule. There are infinite kinds of possible FK crystal structures and so are infinite kinds of FKCH structures.[8] In this section, however, we will show that $\Delta\mu_c$ becomes minimum in only three kinds of crystal structures, CS-I (A15), CS-II (C15), and HS-I (Z), despite the choice of the guest gas molecule. To this end, application of another rule is essential. Yarmolyuk and Kripyakevich found an empirical rule on the numbers of 12-, 14-, 15-, and 16-coordinated atoms in the FK structures.[20] That is, a set of such numbers in any FK crystal structure is given by a linear combination of the three representative crystal structures, A15, C15, and Z. This rule is applicable to all FK structures except for few imaginary structures which have not been found in real alloy materials.[9] For example, the number of 12-, 14-, 15-, and 16-coordinated atoms in σ structure, say $N_{12}^{(\sigma)}$, $N_{14}^{(\sigma)}$, $N_{15}^{(\sigma)}$, and $N_{16}^{(\sigma)}$, are 20, 32, 8, and 0, respectively, and that these numbers can be expressed by the linear combinations of those in A15 ($N_{12}^{(A15)}$, $N_{14}^{(A15)}$, $N_{15}^{(A15)}$, and $N_{16}^{(A15)}$, are 2, 6, 0, and 0) and Z ($N_{12}^{(Z)}$, $N_{14}^{(Z)}$, $N_{15}^{(Z)}$, and $N_{16}^{(Z)}$, are 3, 2, 2, and 0) structures in the following manner:

$$N_k{}^{(\sigma)} = 4N_k{}^{(A15)} + 0N_k{}^{(C15)} + 4N_k{}^{(Z)} \quad (7)$$

where k = 12, 14, 15, or 16. This can be written in a more general form for any FK structure, say A, as

$$N_k{}^{(A)} = p_A{}^{(A15)}N_k{}^{(A15)} + p_A{}^{(C15)}N_k{}^{(C15)} + p_A{}^{(Z)}N_k{}^{(Z)} \quad (8)$$

where $p_A^{(A15)}$, $p_A^{(C15)}$, and $p_A^{(Z)}$ are non-negative constants characteristic to structure A. Equivalently, a set of numbers of 12-, 14-, 15-, and 16-hedral cages in any clathrate hydrate corresponding to the FK structure are expressed by a linear combination of the three representative clathrate hydrate structures, CS-I, CS-II, and HS-I.

Note that 12-, 14-, 15-, and 16-hedral cages have 20, 24, 26, and 28 vertices, respectively, and every vertex belongs to four cages. Therefore, there is a topological relationship between the number of k-hedral cages N_k and the number of vertices (i.e., number of water molecules) N_w as

$$20N_{12} + 24N_{14} + 26N_{15} + 28N_{16} = 4N_w \quad (9)$$

Thus, the linear relation in eq 8 also holds for N_w. Now $\alpha_k^{(A)}$ of any FKCH structure A can be expressed by the linear combination of $\alpha_k^{(CS-I)}$, $\alpha_k^{(CS-II)}$, and $\alpha_k^{(HS-I)}$ in the following manner:

$$\alpha_k{}^{(A)} = \frac{N_k^{(A)}}{N_w^{(A)}}$$

$$= \frac{p_A^{(CS-I)}N_k^{(CS-I)} + p_A^{(CS-II)}N_k^{(CS-II)} + p_A^{(HS-I)}N_k^{(HS-I)}}{p_A^{(CS-I)}N_w^{(CS-I)} + p_A^{(CS-II)}N_w^{(CS-II)} + p_A^{(HS-I)}N_w^{(HS-I)}}$$

$$= \frac{p_A^{(CS-I)}N_w{}^{(CS-I)}\alpha_k^{(CS-I)} + p_A^{(CS-II)}N_w^{(CS-II)}\alpha_k^{(CS-II)} + p_A^{(HS-I)}N_w^{(HS-I)}\alpha_k^{(HS-I)}}{p_A^{(CS-I)}N_w^{(CS-I)} + p_A^{(CS-II)}N_w^{(CS-II)} + p_A^{(HS-I)}N_w^{(HS-I)}} \quad (10)$$

Table 4. Compositions for Various Crystal Structures

FK	CH	$x^{(CS-I)}$	$x^{(CS-II)}$	$x^{(HS-I)}$
A15	CS-I	1	0	0
C15	CS-II	0	1	0
Z	HS-I	0	0	1
σ	TS-I	23/43	0	20/43
μ		0	17/37	20/37
P		23/80	17/80	1/2

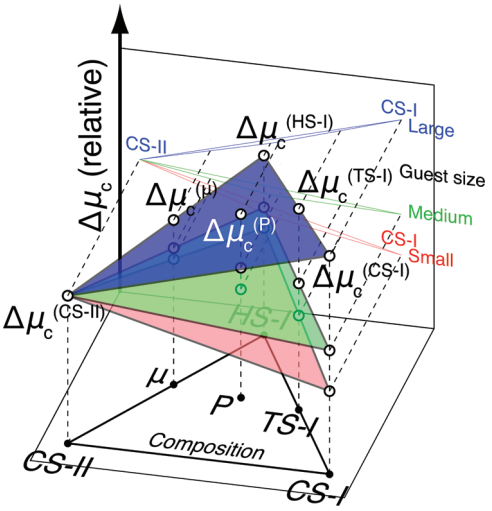

Figure 3. Tilt triangle indicating the partial chemical potentials of water, $\Delta\mu_c$, in height. Three triangles for different guest sizes are shown. The individual heights are offset so as to let the $\Delta\mu_c$ values of CS-II coincide.

Let $x_A^{(CS-I)}$ be defined by

$$x_A{}^{(CS-I)} = \frac{p_A^{(CS-I)}N_w^{(CS-I)}}{p_A^{(CS-I)}N_w^{(CS-I)} + p_A^{(CS-II)}N_w^{(CS-II)} + p_A^{(HS-I)}N_w^{(HS-I)}} \quad (11)$$

then eq 10 can be rewritten simply as

$$\alpha_k{}^{(A)} = x_A^{(CS-I)}\alpha_k^{(CS-I)} + x_A^{(CS-II)}\alpha_k^{(CS-II)} + x_A^{(HS-I)}\alpha_k^{(HS-I)} \quad (12)$$

There is also a simple relation between non-negative $x_A{}^{(CS-I)}$, $x_A{}^{(CS-II)}$, and $x_A^{(HS-I)}$:

$$x_A^{(CS-I)} + x_A^{(CS-II)} + x_A^{(HS-I)} = 1. \quad (13)$$

This allows us to map the FKCH structures inside a triangular diagram (Figure 2). We therefore term x_A "composition". Three vertices of the triangle correspond to the three representative FKCH structures. Compositions for several FKCH structures are listed in Table 4. Thus, we refer to the FKCH structures other than the three representative FKCH structures as "composites". It should be noted that there is no composite structure on the edge connecting A15 and C15, i.e., any FKCH structure other than CS-I and CS-II has 15-hedral cages.[21]

At a glance of $\Delta\mu_c$ in eq 5, the contribution from cage occupancy by a guest species to the chemical potential of water, the argument of the logarithm in eq 5 depends only on the shape of the cage type but is independent of the crystal structures on the assumption that the free energy, f, is dominated by the interaction

dx.doi.org/10.1021/jp203478z |J. Phys. Chem. B 2011, 115, 8257–8265

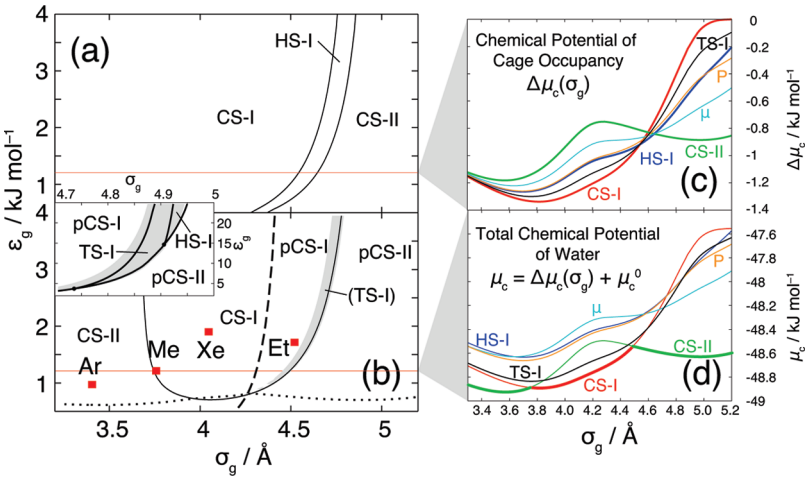

Figure 4. (a) Regions where one of the three representative structures has the lowest $\Delta\mu_c$ among all FKCH structures against LJ parameters σ and ε of the guest molecule. (b) phase diagram of the clathrate hydrate of single component gases against LJ parameters similarly as (a). The regions where TS-I and HS-I are the most stable structure are magnified in the inset. Chemical potential of water in ice and 6 clathrate hydrate structures are calculated to determine the most stable phase. Dashed line stands for the contour where occupancy of dodecahedral cages is 5%. Dotted line is the dissociation limit. Red dots correspond to the LJ parameters of guest gases. Shaded area indicates the region where difference in the chemical potential between TS-I and the most stable structure is less than 50 J mol^{-1}. (c) and (d) the cross sections at ε_g = 1.2355 kJ mol^{-1}, (of methane) for $\Delta\mu_c$ the contribution from the cage occupancy and μ_c the total chemical potential of water. The lower envelope of μ_c (bold line) indicates the most stable structure at the given guest size.

with water molecules making up the cage. Therefore, $\Delta\mu_c$ of any FKCH structure is also expressed by the linear combination of $\Delta\mu_c$ of the three representative structures as

$$\Delta\mu_c^{(A)} = x_A^{(CS\text{-}I)}\Delta\mu_c^{(CS\text{-}I)} + x_A^{(CS\text{-}II)}\Delta\mu_c^{(CS\text{-}II)} + x_A^{(HS\text{-}I)}\Delta\mu_c^{(HS\text{-}I)} \quad (14)$$

That is, $\Delta\mu_c$ of all the FKCH structures are coplanar; they are inside the tilt triangle $\Delta\mu_c^{(CS\text{-}I)} - \Delta\mu_c^{(CS\text{-}II)} - \Delta\mu_c^{(HS\text{-}I)}$ (Figure 3).

It must be stressed that the chemical potential of the guest μ and the "fitness" f in eq 5 are independent of crystal structure; that is, it is impossible to stabilize a specific composite structure by controlling gas pressure, by changing composition of the gas mixture, or by choosing the guest species. Any such attempt merely changes the slope of the triangle leaving one of three representative structures the most stable (Figure 3). This can be explained as follows. Among all the FKCH structures, CS-I has the largest number of 14-hedral cages per the number of water molecules, CS-II has the largest number of 12- and 16-hedral cages, and HS-I has the largest number of 15-hedral cages. They are extrema in number of these cages. If one attempts to stabilize a composite FKCH structure by choosing the guest molecule(s) which fits in the k-hedral cage, one of three extremal structure is always more stable than the composite FKCH because it has more k-hedral cages than the composite FKCH structure. In the present work, the polyatomic molecules are approximated to be spherical molecules. As far as the assumptions of vdWP theory are effective, the error due to the approximation on the molecular shape acts equivalently to the free energies of all the Frank-Kasper type clathrate hydrates; that is, it may tilt the triangle in Figure 3, but the phases are expected to remain coplanar.

Then, a question arises as to which conditions make one of three representative structures to have the lowest $\Delta\mu_c$. In Figure 4a, a phase diagram where the region of the representative structures has the lowest $\Delta\mu_c$ is shown against the LJ parameters of the guest molecule. One can see that HS-I occupies very narrow area. It is because HS-I has the lowest $\Delta\mu_c$ only when the guest molecule just fits to 15-hedral cage. The difference in $\Delta\mu_c$ to the second lowest CS-I for spherical molecule is at most 138 J mol^{-1} within the area of Figure 4a. Note that the difference becomes larger for the guest molecule like bromine that interacts stronger with water, which will be discussed in the later section. Most of the molecules having larger or smaller size prefer CS-II or CS-I, respectively.

E. Free Energy of the Empty Clathrate Hydrate. The chemical potential of cage occupancy, $\Delta\mu_c$, dominates in preferential formation of a specific structure depending implicitly on both the cage-type and the free energy of cage occupancy, f, while the chemical potential of the empty clathrate μ_c^0 usually plays a minor role despite its magnitude. The contribution from the host lattice, μ_c^0, can be a key for such selection in case of competing $\Delta\mu_c$ of two structures. Such a competition occurs (1) when the guest molecule is so small that it fits to any cage size, (2) when the guest molecule is too large to fit to any cage type, or (3) around the boundaries shown in Figure 4a.

In classical harmonic approximation, the chemical potential of the hypothetical empty clathrate hydrate in the limit of low pressure is decomposed into two terms

$$\mu_c^0 = u + f^{(h)} \quad (15)$$

where u is the potential energy at 0 K and $f^{(h)}$ is the harmonic free energy of lattice vibration.[14]

The latter term is obtained by normal-mode analysis of the hypothetical empty clathrate hydrate structure at 0 K in the following equation:

$$f^{(h)} = k_B T \sum_i^{6N_w - 3} \ln(\beta\hbar\omega_i)/N_w \quad (16)$$

where ω_i is the ith normal mode angular frequency and the summation is carried out over real positive ω_i. The anharmonic free energy is relatively small compared with any other contribution.[22]

dx.doi.org/10.1021/jp203478z |J. Phys. Chem. B 2011, 115, 8257–8265

Table 5. Potential Energy and Free Energy of Ice and Various Clathrate Hydrate Crystal Structures

FK	CH	u/kJ mol^{-1}	$f^{(h)}$/kJ mol^{-1}	$u + f^{(h)}$/kJ mol^{-1}	x_6
Ice Ih		−55.22	+6.94	−48.29	
C15	CS-II	−54.78	+7.03	−47.74	0.118
A15	CS-I	−54.39	+6.83	−47.55	0.13
σ	TS-I	−54.37	+6.84	−47.54	0.128
μ		−54.02	+6.61	−47.41	0.122
P		−54.21	+6.81	−47.40	0.125
Z	HS-I	−54.33	+6.96	−47.37	0.125

Since our concern is the free energy difference among various clathrate structures, it is reasonable to consider the anharmonic contribution is similar to each other and thus ignore it. The magnitude of the residual entropies due to the proton-disorder is common to all crystalline phases. Hereafter no consideration of its contribution to the free energy is taken into. Since we deal with those ice-like crystals at low pressures, the pressure term in the free energy is always small. When comparison is made among various FKCH structures, differences among them are expected to be much smaller.

All of the FKCH structures consist of 12- to 16-hedra in which tetrahedral local configuration of water molecules is almost undistorted. Therefore, the potential energies of these structures are comparable (so are clathrate structures of silicon and germanium[23]). In fact, the small difference in μ_c^0 becomes important when the difference in $\Delta\mu_c$ is small. In Table 5, the potential energies and vibrational free energies of ice and various empty clathrate hydrate structures are listed. In the present model, CS-II is found to have the lowest μ_c^0 and CS-I has the second lowest followed by TS-I. Our calculation for free energy difference between CS-I and CS-II reasonably reproduces the experimental result.[24] When the guest molecule is much smaller than the cage size, for example, $\Delta\mu_c$ is comparable in any structure and that the CS-II structure having the lowest μ_c^0 value is the most stable. μ_c^0 value of HS-I is much higher compared with that for CS-I and CS-II.

A possible reason for the difference in the lattice free energy among various clathrate hydrate structures is the number of 6-membered rings.[25] In clathrate hydrates, the oxygen−oxygen−oxygen angle on the 6-membered ring is 120°, which is fairly distorted from the tetrahedral value of 109.5°. Hence, the more 6-membered rings a clathrate structure has, the more it becomes unstable. To examine this intuitive view in more detail, the number of 6-membered rings per a water molecule in the clathrate hydrate structure x_6, defined as

$$x_6 = \frac{2N_{14} + 3N_{15} + 4N_{16}}{2N_w} \tag{17}$$

is compared with the potential energy. x_6 values thus defined are listed in Table 5. There is no clear correlation between x_6 and the potential energy. For example, HS-I has the intermediate x_6 value between CS-I and CS-II, while its lattice energy is higher than that either of the two structures. Therefore the number of 6-membered rings is not fully responsible to the lattice energy difference. We further explore the correlation between the lattice energy and various topological information in Tables 1 and 4, but no simple relation is found. It should be explained rationally in terms of the packing of the polyhedral cages and the overall distortion of the HB network. Although we cannot foresee the relative stability of empty clathrate hydrates derived from the FK structures, it is a simple task to calculate the free energy of empty structure which can be a candidate for a new stable clathrate structure according to eq 15.

F. Phase Diagram. The chemical potential of water in various clathrate hydrate structures with single component gases is calculated on the basis of the theory developed in the previous sections. The phase diagram is given against the LJ parameters of the guest molecule in Figure 4b. In both experiments and simulations, it is known that the crystal structure changes from CS-II to CS-I, then partially occupied CS-I (pCS-I) takes over, and finally partially occupied CS-II (pCS-II) is recovered as the size of the guest molecule increases.[25−27] A host lattice structure seems to be, however, rather insensitive to LJ ε value appropriate to simple hydrocarbons and noble gases.

An important prediction is that there may be a very narrow region between pCS-I and pCS-II in the phase diagram where TS-I (FK σ phase) is the most stable, as shown in the inset of Figure 4b. TS-I can be the most stable when $\Delta\mu_c$ of HS-I is much lower than that of CS-I and CS-I is more stable than CS-II. In such a case, TS-I must appear on the CS-I side of CS-I to CS-II coexistence line in the phase diagram. It is difficult to identify TS-I as the most stable phase because of the approximations made in the present theory. Instead, we estimate the region in the phase diagram where the difference in μ_c between the most stable phase (CS-I or CS-II) and TS-I is very small, which is indicated by gray in Figure 4b. Then, stability order in this region may alternate by a small error which arises from flaws in the description of the intermolecular interactions and/or in the approximations made in our free energy calculation. In addition, our theoretical calculation also predicts the emergence of HS-I when the guest−host interaction is very strong. However, such a strong interaction may destabilize the host lattice.[28]

It must be stressed that the partial chemical potentials of water, $\Delta\mu_c$, of all 6 FKCH structures come close to each other at the phase boundary between pCS-I and pCS-II as shown in Figure 4c, that is, the tilt triangle of $\Delta\mu_c$ in Figure 3 becomes almost horizontal. Although only 6 different FKCH structures are examined in the present work, all other FKCH structures must also have the corresponding $\Delta\mu_c$ value with each other at the point. Actually, the total chemical potentials of water, μ_c, of 6 FKCH structures also get closest at the point as shown in Figure 4d. This suggests that one should search for a new clathrate hydrate structure around the phase boundary between pCS-I and pCS-II. In this way, we may explore the appropriate parameters of model guest species for a specific structure to be the most stable, taking advantage of the fact that changing parameters simply alters the slope of the triangle for the partial chemical potential of water $\Delta\mu_c$ and that for any FKCH structure falls into the triangle.

G. Bromine Hydrate. Bromine is the only exceptional guest species that stabilizes a clathrate hydrate structure known as TS-I structure instead of CS-I or CS-II.[29] Moreover, when the TS-I crystal is exposed to excess water at a temperature below 266 K, the CS-II crystal forms on the surface.[30] It implies that the TS-I crystal of bromine hydrate exists in a very narrow range of thermodynamic condition. We will apply our theory developed here to estimate the structure selectivity of bromine hydrate at 273 K. A bromine molecule is treated as a diatomic (dumbbell-like) molecule rather than a single interaction site in order to avoid inaccuracy caused by the long Br−Br bond. The free energy of cage occupancy for a diatomic molecule is

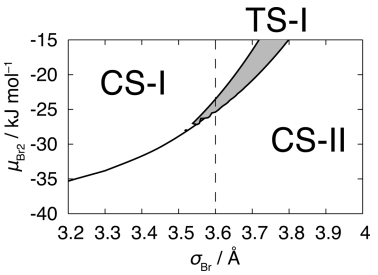

Figure 5. Phase diagram of the bromine hydrate plotted against the atomic diameter and chemical potential of bromine. Dashed line indicates the original atomic diameter of the present model.

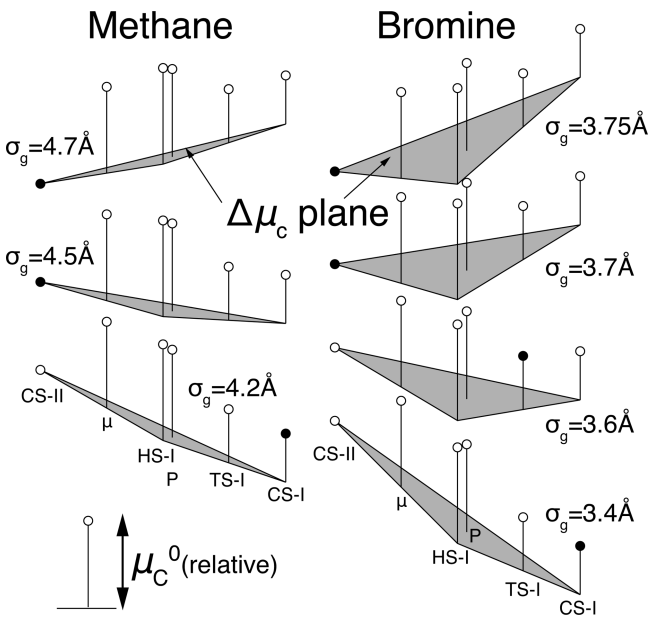

Figure 6. $\Delta\mu_c$ planes, exemplified in Figure 3, drawn for methane-like and bromine-like molecules with various molecular sizes. The height of the vertical line from the triangle correspond to the chemical potential of water in the hypothetical empty hydrate, μ_c^0, relative to that of CS-II. Height of the circle gives a schematic presentation of the stability of the structure, i.e., total chemical potential of water, $\mu_c = \mu_c^0 + \Delta\mu_c$. Black circle indicates the most stable structure at the given molecular size.

calculated by

$$f = -k_B T \ln[\frac{1}{\sigma}(Ik_B T/2\pi\hbar^2)(mk_B T/2\pi\hbar^2)^{3/2} \int\int_{V_{cage}} \exp(-\beta w(\mathbf{r},\Omega))\, d\mathbf{r}\, d\Omega] \quad (18)$$

where I and σ are moment of inertia and the symmetry number, respectively, and integration is carried out over all positions and orientations of a guest inside a given cage. Note that eq 3 is not applicable to calculate the chemical potential of bromine because bromine is in liquid phase at the temperature. Instead, the chemical potential of bromine, μ_{Br2}, is treated here as an independent variable.

The LJ parameters of bromine atom are reported to be σ_g = 3.60 Å and ε_g = 1.413 kJ mol^{-1}, and the bond length L is 2.28 Å.[31] As is shown in Figure 4, structure of the clathrate is determined mainly by the molecular size and is insensitive to LJ ε_g parameter. Therefore, the size (atomic diameter of bromine) dependency is

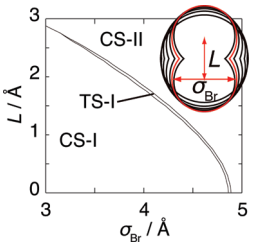

Figure 7. Phase diagram of the clathrate hydrate of a diatomic molecule plotted against the atomic diameter σ_g and bond length L. The inset picture illustrates the molecular geometries when TS-I is the most stable.

examined over a certain range of LJ σ_g around the above value with the fixed bond length L and LJ ε_g. In Figure 5, phase diagram of bromine hydrate is plotted against atomic diameter σ_g and chemical potential μ_{Br2} of bromine. It indicates that there is a narrow region between CS-I and CS-II where TS-I crystal is the most stable. When the chemical potential of bromine decreases, cage occupancy of bromine also decreases, and the stability of the hydrate is dominated by the chemical potential of the host lattice. CS-II is the most stable when the cages are less occupied, which agrees with experimental observation that bromine hydrate exposed to excess water transforms to CS-II.[30] Figure 6 illustrates how the most stable structure is selected. Stability of a structure is determined by the chemical potential of water in eq 4, which is sum of μ_c^0 and $\Delta\mu_c$. The former is a constant for each crystal structure at the given temperature, while the latter is on a plane, as shown previously. The slope of the $\Delta\mu_c$ plane is large if the guest−host interaction is strong. In case of methane, weak interaction between methane and water yields only a small slope of the plane leaving either CS-I or CS-II the most stable structure. Strong interaction between bromine and water subducts the HS-I vertex of the triangle, which consequently stabilizes TS-I. (Much stronger guest−host interaction may even make the chemical potential in HS-I structure the lowest.)

One may think that a rod-like bromine molecule specifically fits to the prolate 15-hedral cage, and that stabilizes the clathrate structures having 15-hedral cages such as TS-I and HS-I. However, it is found that the molecular shape is not the decisive factor. The phase diagram pertinent to molecular shape is drawn in Figure 7 against the atomic diameter σ_g and the bond length L with the fixed LJ ε_g parameter to the original value of the model and at the chemical potential μ_{Br2} = −25 kJ mol^{-1}. It shows that TS-I phase is the most stable at an appropriate diameter even if the bond length L is zero, which is consistent with Figure 4b.

H. Case of Multicomponent Gases. It is shown that only the two representative structures, CS-I and CS-II, can be stable as a clathrate hydrate containing single guest species among many possible FKCH structures, which is consistent with the experimental observations. Then, a question naturally arises: is it possible for the other structures than CS-I or CS-II to yield in nature by increasing the number of gas components? Unfortunately, it is shown that a new clathrate structure suggested by the FK structures other than CS-I or CS-II cannot be observed within the vdWP theory except for a small region suggested in Figure 4. The logarithmic term in eq 5 is independent of the crystal type upon a given gas-composition. According to the vdWP theory, the lattice energy is also independent of the guest species. Consequently, even the multicomponent gases do not form any new clathrate hydrate structure located inside the triangle in Figure 2 given that single component gas fails to form it.

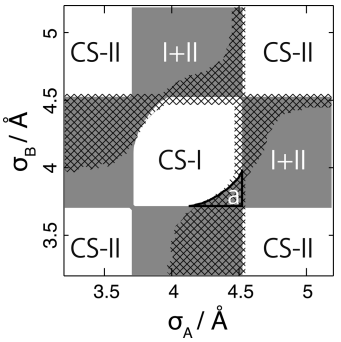

Figure 8. Phase diagram of 2-component gas clathrate hydrate mapped against the guest molecular sizes. In the gray region, the crystal structure changes from CS-I to CS-II depending on the partial pressure of the gases. In the crosshatched region, the free energy difference between TS-I and the most stable phase is smaller than 50 J mol^{-1} at an appropriate partial pressure where the total pressure is set to 10 MPa and other parameters are fixed at the value of ethane. In the region "a", mixing of two gases yields CS-II structure even though each component gas prefers CS-I structure. [ref 10].

In case of the single-component gas, as we note in the previous section, TS-I and HS-I may become the stable phase around the phase boundary between CS-I and CS-II where the chemical potentials of the two phases compete. We may search for a new structure located on the edges of the triangle in Figure 2 (and the vertex HS-I). It is, however, not easy to change the size and interactions of the real guest molecule to target the phase boundary. One can circumvent this difficulty by replacing a single component of guest with gas mixtures. A competition in the chemical potential of water is expected to occur in a wide range of guest molecular sizes if proper partial pressures (or compositions) are given. A simple example of clathrate hydrates containing two component gases is shown in Figure 8. In the case of chemical potential of water competes, there might be the other origins, even though small, to alternate the order of stability according to the vdWP theory, i.e., some missing components of the free energy within the original vdWP theory such as the guest anisotropy, the anharmonic contribution, and the free energy change of the host lattice in the presence of guest molecules.

III. CONCLUSIONS

We successfully account for the structure selectivity of the clathrate hydrates by the vdWP theory combined with Yarmolyuk-Kripyakevich empirical rule as:

1 According to $\Delta\mu_c$, one of the three representative structures, CS-I, CS-II, and HS-I, gives the lowest $\Delta\mu_c$ values among all possible FKCH structures, depending on the guest species.
2 CS-I and CS-II give low value of μ_c^0 compared with HS-I.
3 Consequently, only two structures, CS-I and CS-II, are the most stable structures at ambient conditions.
4 TS-I is an exception, which possibly appears at the phase boundary between CS-I and CS-II.

These theoretical calculations are supported by experimental observations that no other hydrate structure with a single guest component has been found at an ambient condition (except for bromine) and the structural change takes place in some clathrate hydrates in equilibrium with a multicomponent gas in a certain range of composition. It is also indicated that TS-I is a candidate for the second most stable clathrate hydrate structure. On the other hand, HS-I is found to be less stable because its free energy of empty clathrate is relatively high.

When the chemical potential of cage occupancy, $\Delta\mu_c$, of the two representative clathrate hydrate structures, say CS-I and HS-I, coincide, all the composite FKCH structures between them also have the same chemical potential and that new clathrate hydrate structures might be possibly found near the phase boundary between the representative clathrate hydrate structures (in Figures 4–6 and 8). In experiments, it is impossible to control the molecular size continuously and that it is difficult to satisfy the condition where the free energies for some structures compete. Instead, it is rather easier to access the phase boundary between pCS-I and pCS-II by changing the partial pressure of the multicomponent gases. Competition of multiple phases may hinder crystallization, which is useful in case when crystallization is undesirable.

In the present approximation, the chemical potential of empty clathrate hydrate, μ_c^0, is assumed to be irrelevant to the guest molecule type. This approximation will be more appropriate for silica and silicon clathrates where the host–host interaction is much stronger.[32] On the other hand, if the lattice frequencies are affected by the existence of the guest molecules, it may change μ_c^0 and thus alternate the order in stability. Such a guest species may bring us undiscovered clathrate hydrate structures.

In the present work, only the clathrate hydrates having the cages consist of pentagonal and hexagonal faces, i.e. FKCH, are taken into consideration, because Yarmolyuk-Kripyakevich's rule is applicable to them. To construct more general theory on the structure selectivity of clathrate hydrates, one must find additional topological rules comprising 4- and 7-member rings of the HB network.

Present theory elucidates the existence of many metastable crystal structures. Ostwald's step rule simply states that the less stable structure appears first at the crystallization, but does not mention the structure selectivity if many metastable structures exist.[33] Some of them are similar in structure and symmetry and that it is possibly easy to change from one to another with small energy barriers. In order to control the crystallization via metastable phases and to develop the methodology of producing the new clathrate hydrate structures, we must learn the proximity network of reaction pathways between metastable phases.

AUTHOR INFORMATION

Corresponding Author

*Phone: +81-86-251-7846. E-mail: vitroid@gmail.com.

ACKNOWLEDGMENT

The authors are grateful to Dr. Lukman Hakim for critical readings of the manuscript. This work was supported in part by Grant-in-Aid from JSPS, Next Generation Supercomputer program.

REFERENCES

(1) Davidson, D.W. In *Water—A Comprehensive Treatise*; Franks, F., Ed.; Plenum: New York, 1973; Vol. 2.
(2) Sloan, E. D. *Clathrate Hydrate of Natural Gases*; Marcel Dekker, Inc.: New York, 1998.
(3) Udachin, K. A.; Enright, G. D.; Ratcliffe, C. I.; Ripmeester, J. A. *J. Am. Chem. Soc.* **1997**, *119*, 11481–11486.

(4) Miller, S.; Gough, S. R.; Davidson, D. W. *J. Phys. Chem.* **1977**, *81*, 2154–2157.
(5) Yang, L.; Tulk, C. A.; Klug, D. D.; Moudrakovski, I. L.; Ratcliffe, C.; Ripmeester, J.; Chakoumakos, B. C.; Ehm, L.; Martin, C. D.; Parise, J. B. *Proc. Natl. Acad. Sci. U.S.A.* **2009**, *106*, 6060–6064.
(6) Hakim, L.; Koga, K.; Tanaka, H. *Phys. Rev. Lett.* **2010**, *104*, 115701.
(7) Matsumoto, M. *J. Phys. Chem. Lett.* **2010**, *1*, 1552–1556.
(8) Frank, F. C.; Kasper, J. S. *Acta Crystallogr.* **1959**, *12*, 483–499.
(9) Sikirić, M. D.; Delgado-Friedrichs, O.; Deza, M. *Acta Crystallogr.* **2010**, *A66*, 602–615.
(10) Koyama, Y.; Tanaka, H.; Koga, K. *J. Chem. Phys.* **2005**, *122*, 074503.
(11) Local packing fraction of the spheres of unit diameter placed at the vertices of a regular n-hedron is calculated by $\eta_n = \nu_n\omega_n/24V_n$, where ν_n, ω_n, and V_n are the number of vertices, solid angle of a vertex and the volume of a unit n-hedron, respectively. Note that η_n is 0.7796 for a tetrahedron and 0.7209 for an octahedron. Rogers, C. A. *Proc. London Math. Soc.* **1958**, *s3−8*, 609–620.
(12) Sadoc, J.-F.; Mosseri, R. *Geometrical Frustration*; Cambridge University Press: Cambridge, U.K., 1999.
(13) Tanaka, H.; Kiyohara, K. *J. Chem. Phys.* **1993**, *98*, 8110–8118.
(14) Tanaka, H.; Kiyohara, K. *J. Chem. Phys.* **1993**, *98*, 4098–4109.
(15) The Alloy database http://alloy.phys.cmu.edu/alloydb.copy/alloydb/adbhtml/MoNi.oP56.28Mo-28Ni.PAW_GGA.html.
(16) Tanaka, H. *Fluid Phase Equilib.* **1998**, *144*, 361–368.
(17) van der Waals, J. H.; Platteeuw, J. C. *Adv. Chem. Phys.* **1959**, *2*, 1–57.
(18) Hirschfelder, J. O.; Curtiss, C. F.; Bird, R. B. *Molecular Theory of Gases and Liquids*; Wiley: New York, 1954.
(19) Jorgensen, W. L.; Chandrasekhar, J.; Madura, J. D.; Impey, R. W.; Klein, M. L. *J. Chem. Phys.* **1983**, *79*, 926.
(20) Yarmolyuk, Y. P.; Kripyakevich, P. I. *Sov. Phys. Crystallogr.* **1974**, *19*, 334–337.
(21) Hellner, E.; Pearson, W. B. *J. Solid State Chem.* **1987**, *70*, 241–248.
(22) Tanaka, H. *J. Chem. Phys.* **1994**, *101*, 10833.
(23) O'Keeffe, M.; Adams, G. B.; Sankey, O. F. *Philos. Magazine Lett.* **1998**, *78*, 21–28.
(24) Handa, Y. P.; Tse, J. S. *J. Phys. Chem.* **1986**, *90*, 5917.
(25) Jacobson, L. C.; Hujo, W.; Molinero, V. *J. Phys. Chem. B* **2009**, *113*, 10298–10307.
(26) Sloan, E. D., Jr. *Gas Hydrates: Relevance to World Margin Stability and Climate Change*; Geol. Soc: London, 1998.
(27) Jacobson, L. C.; Molinero, V. *J. Phys. Chem. B* **2010**, *114*, 7302–7311.
(28) Koga, K.; Tanaka, H.; Nakanishi, K. *Mol. Simul.* **1994**, *12*, 241–252.
(29) Allen, K. W.; Jeffrey, G. A. *J. Chem. Phys.* **1963**, *38*, 2304–2305.
(30) Goldschleger, I. U.; Kerenskaya, G.; Janda, K. C.; Apkarian, V. A. *J. Phys. Chem. A* **2008**, *112*, 787–789.
(31) Jolly, D. L.; Freasier, B. C.; Hamer, N. D.; Nordholm, S. *Chem. Phys.* **1984**, *88*, 261–270.
(32) Momma, K.; Ikeda, T.; Nishikubo, K.; Takahashi, N.; Honma, C.; Takada, M.; Furukawa, Y.; Nagase, T.; Kudoh, Y. *Nat. Commun.* **2011**, *2*, 196–197.
(33) Ostwald, W. *Z. Phys. Chem.* **1897**, *22*, 289–330.